Tables S1-S8
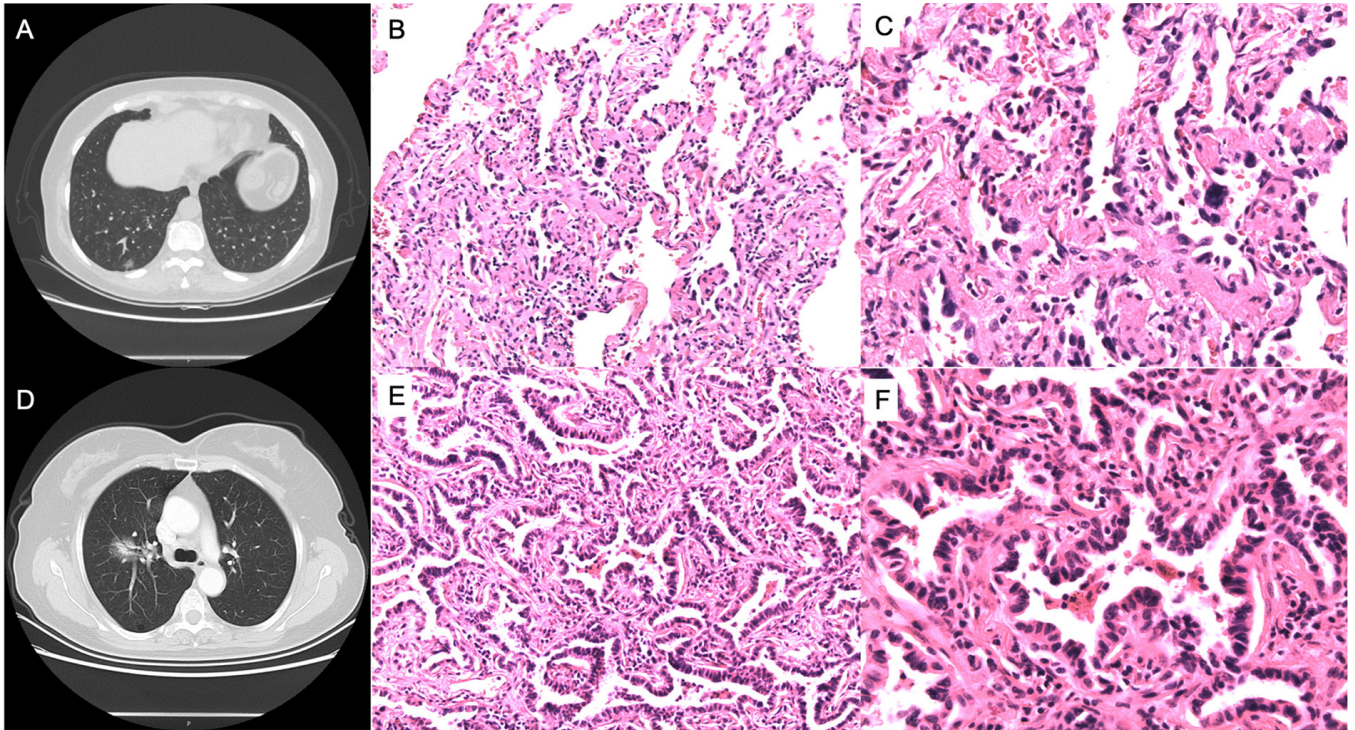
Available at https://cdn.amegroups.cn/static/public/tlcr-20-1086-table S1-S8.xlsx


Figure S1 Computed tomography (CT) image and Hematoxylin-eosin (HE) staining of different GGN subtypes. (A) CT image showing a case of peripheral pure ground-glass nodule (GGN) of the right lower lobe. (B,C) Photomicrograph of a case of adenocarcinoma with predominant lepidic pattern (HE stain, ×100 and ×200, respectively). (D) CT image showing a case of centrally located, part-solid nodule of the right upper lobe. (E,F) Photomicrograph of a case of adenocarcinoma with predominant acinar pattern (HE stain, ×100 and ×200, respectively).
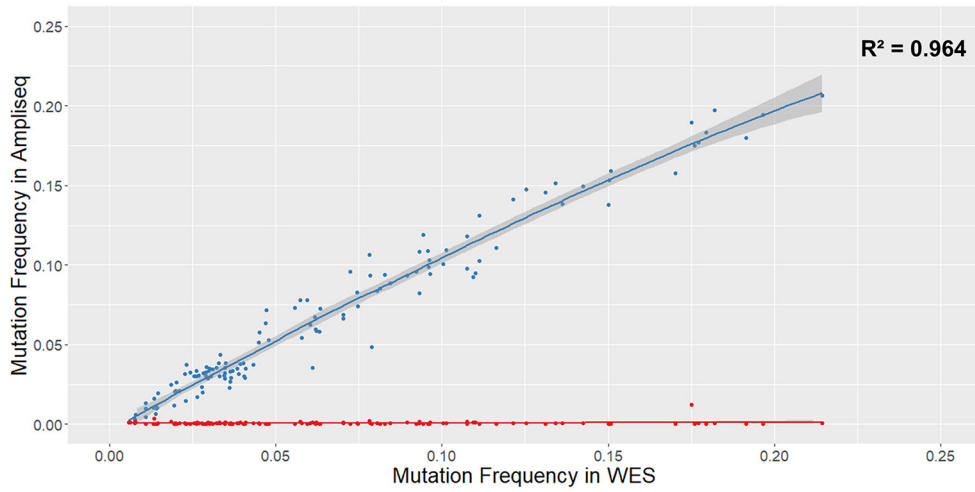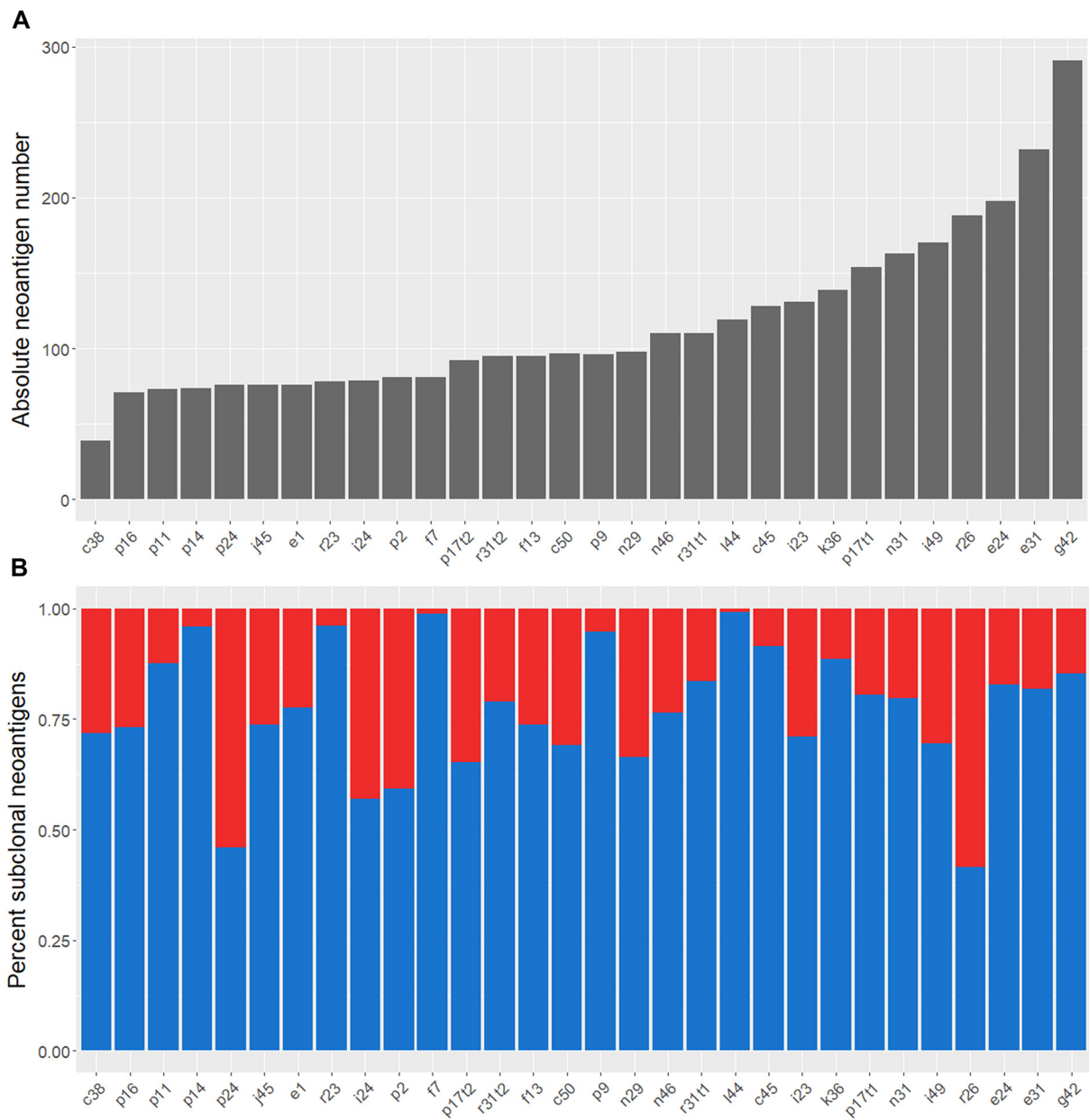
Figure S2 Pearson correlation between mutated allele frequency calling from the WES and the amplicon deep sequencing. Blue and red dots depict the mutated allele frequency of selected SNVs calling from amplicon deep sequencing tumor and normal samples, respectively. The 130 SNVs calling from p9, p11, p14 and p17t2 WES data were randomly selected for this analysis.
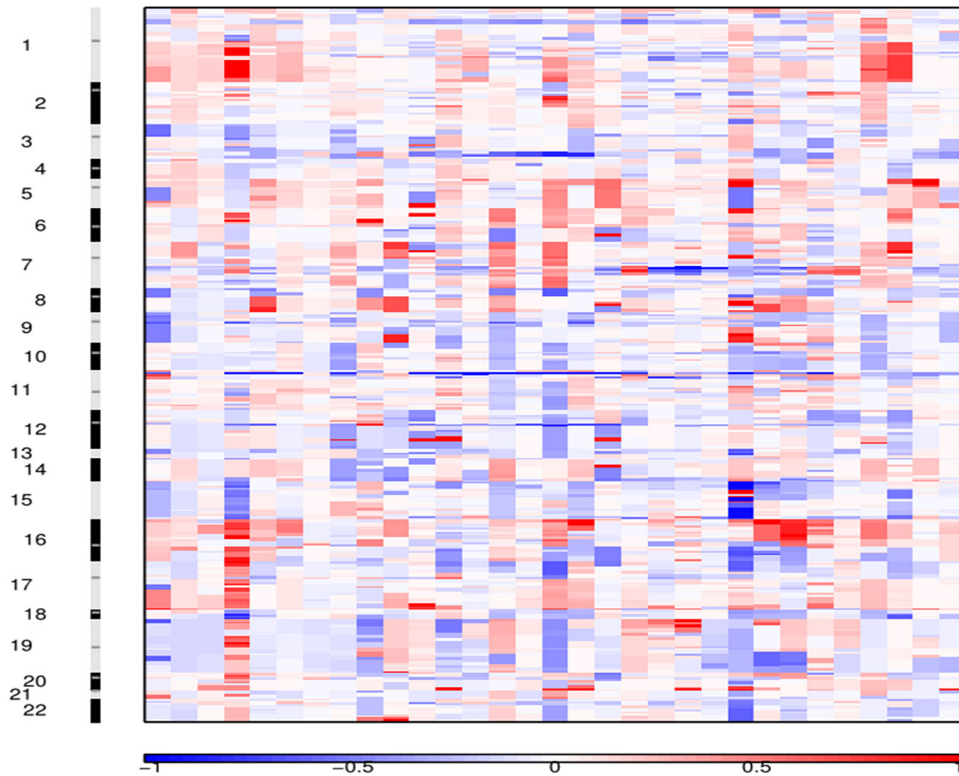
Figure S3 The heatmap showing the segmented copy-number profiles in GGNs. The chromosomes are arranged vertically from top to bottom and samples are arranged from left to right. Red and blue represent gain and loss, respectively.
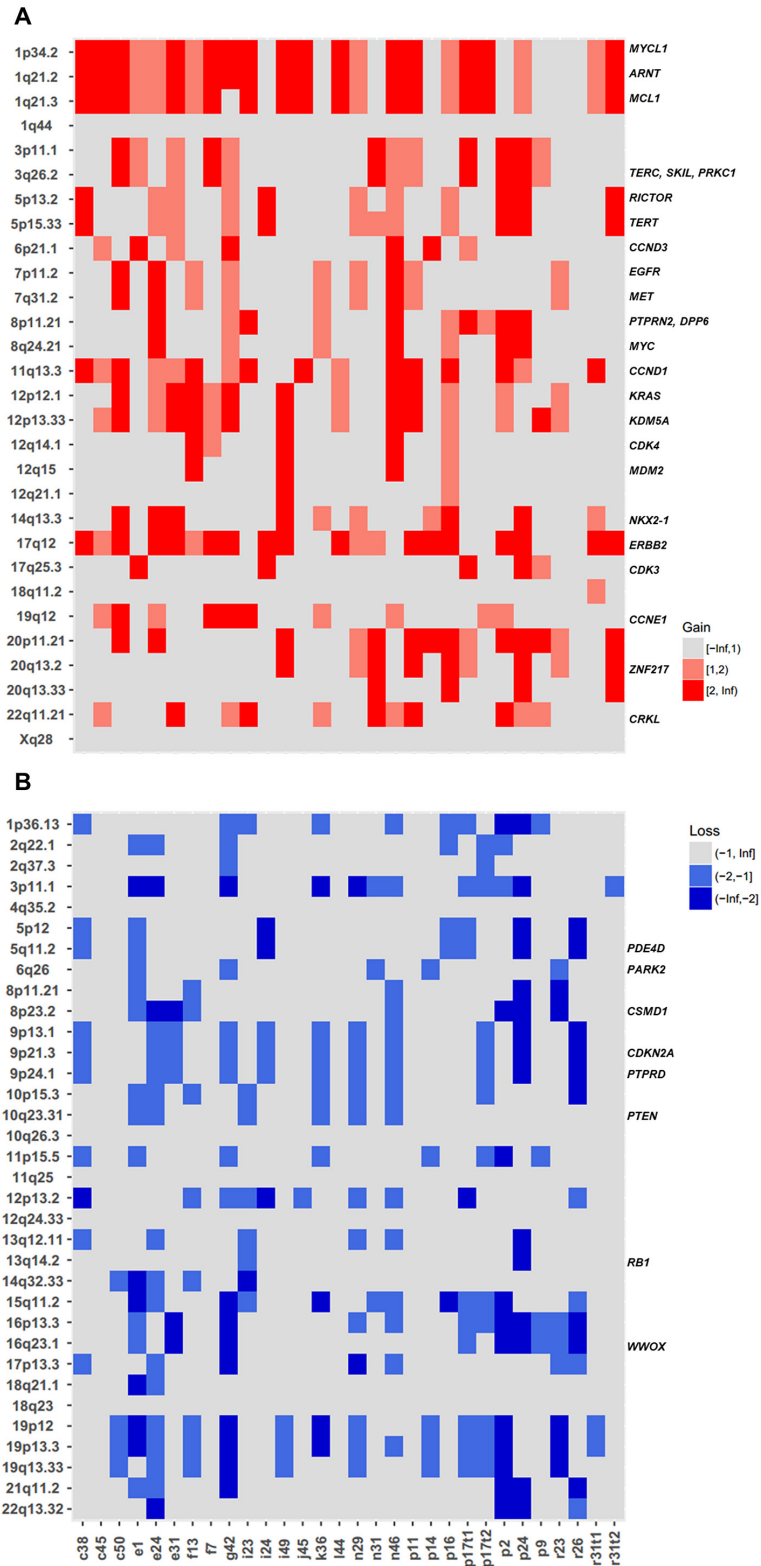
Figure S4 The heatmap showing copy number changes in known recurrently altered regions in LUAD. (A) Light red represents gain of one copy relative to the ploidy, while dark red represents gain of ≥2 copies relative to the ploidy. (B) Light blue represents loss of one copy relative to the ploidy, while dark blue represents loss of ≥2 copies relative to the ploidy.

Figure S5 The neoantigen landscape in GGNs. (A) The neoantigen burden in each GGN. (B) The percentages of neoantigens that were found to be clonal or subclonal in each GGN.

Figure S6 Pearson correlation between neoantigen burden and exonic mutation burden among GGNs. R^2 depicts the squared Pearson correlation coefficient.